Available online at www.sciencedirect.com
SCIENCE DIRECT®
Spectrochimica Acta Part B 58 (2003) 1019–1030
SPECTROCHIMICA ACTA PART B
www.elsevier.com/locate/sab

# Slow muon experiment by laser resonant ionization method at RIKEN-RAL muon facility☆

P. Bakule[a,b,*], Y. Matsuda[a,b], Y. Miyake[c], P. Strasser[a], K. Shimomura[a], S. Makimura[c], K. Nagamine[c]

[a]*Muon Science Laboratory, RIKEN (The Institute of Physical and Chemical Research), Wako, Saitama 351-01, Japan*
[b]*RIKEN Muon Facility, Rutherford Appleton Laboratory, ISIS R3, Chilton OX110QX, UK*
[c]*Meson Science Laboratory, High Energy Accelerator Research Organization (KEK), 1-1 Oho, Tsukuba, Ibaraki 305-0801, Japan*

Received 7 July 2002; accepted 31 January 2003

**Abstract**

We report first results of the slow muon generation from pulsed surface muon beam using a method of resonant laser ionization of muonium. The muonium is produced from the muon beam by electron capture near the surface of thin tungsten foil heated to 2100 K. The ionization is resonantly enhanced by using a vacuum-ultraviolet (VUV) radiation resonant with 2P state of muonium ($\lambda_{1S-2P}=122.09$ nm). A pulsed beam at 355 nm is used for an efficient ionization from the 2P state. The VUV beam with pulse duration of 4 ns and with bandwidth of over 100 GHz to match the Doppler broadening of muonium (200 GHz) is generated by resonant third-order sum-difference frequency conversion ($\omega_{VUV}=2\omega_R-\omega_T$) in krypton gas phase-matched with argon buffer gas. The $\omega_R$ beam has been tuned to the two-photon resonance of $4p^5 5p[1/2,0]$ state in krypton to enhance the conversion process. Yield of the VUV radiation has been investigated for different energies and confocal parameters of the incident beams. The whole apparatus, including a beamline for transport and detection of ionized particles, has been tested by ionizing residual hydrogen atoms at an ultra-high vacuum level of $1.1\times10^{-9}$ hPa with efficiency better than $10^{-3}$. The yield of slow muons obtained during the first beamtime was 0.03 $\mu^+$/s.


*Keywords:* Vacuum-ultraviolet beam; Infrared; Optical parametric oscillators; Muon; Muonium

## 1. Introduction

A slow muon beam with energy below 100 eV that can be accelerated to energies in the range of 2–10 keV can provide an excellent tool for condense matter physics extending the scope of muon spin relaxation technique from bulk materials to thin samples. The penetration depth of muons at these very low energies can range from the sub-nanometre to several nanometre region. This allows for systematic studies of thin films, multi-layered structures, nanomaterials and extremely small samples. There have been several proposed

☆ This paper was presented at the International Conference on Laser Probing (LAP-2002), held in Leuven, Flanders, Belgium, July 2002, and is published in the Special Issue of *Spectrochimica Acta Part B*, dedicated to that conference.

*Corresponding author. Tel.: +44-1235-445256; fax: +44-1235-446881.
*E-mail address:* p.bakule@rl.ac.uk (P. Bakule).

0584-8547/03/$ - see front matter © 2003 Elsevier Science B.V. All rights reserved.
doi:10.1016/S0584-8547(03)00062-4

methods of slow muon generation [1]. In terms of the beam intensity, the muon moderation technique developed at PSI has been so far the most successful [2]. This technique produces polarized muons with energies below 30 eV, with a broad peak centered at 15 eV. An alternative method we are investigating potentially produces muons with energy as low as 0.2 eV (ultra-slow muons). The method is based on the laser ionization of muonium atoms ($\mu^+e^-$) in ultra-high vacuum. The muonium can be produced with high conversion efficiency (1–4%) by stopping high energy, 4 MeV surface muon beam in thin tungsten foil heated to 2100 K [3]. The muonium is formed by electron capture near the surface of the hot foil. The muonium atoms can then escape to the vacuum with thermal velocity.

Using a pulsed Lyman-α (122 nm) laser system the muonium is resonantly excited from 1S ground state to 2P state and subsequently photoionized with a 355 nm laser beam. The ultra-slow muons are then extracted and accelerated in a static electric field. The method of muonium ionization was first successfully tested at the pulsed proton beamline at Meson Science laboratory of the High Energy Accelerator Research Organization (KEK) in Japan [4]. The thermal muonium was produced directly in the 500 MeV proton beam from a composite target consisting of boron nitride pion production target and a heated tungsten foil. However, there are serious technical issues associated with the radiation in the primary proton beamline limiting more systematic study of optimum conditions for the muonium production. We have therefore decided to take advantage of a high intensity pulsed surface muon source available at RIKEN-RAL beamline at ISIS facility of Rutherford Appleton Laboratory, UK. A new experimental setup consisting of a laser system for muonium ionization operating with a repetition rate of 25 Hz, a muonium production target, and an ultra-slow muon beamline was installed at Port 3 of RIKEN-RAL facility, where $5\times10^5$ surface muons/s are available in a beam pulsed at 50 Hz and with a pulse duration of 80 ns [5]. In this progress report we are presenting the details of our laser system and first results of the ultra-slow muon generation at RIKEN-RAL.

The muonium ionization efficiency is currently limited by the availability of sufficiently intense Lyman-α source. The 1S–2P transition is strongly allowed electric dipole transition with saturation intensity of only 2.3 $W/cm^2$ over a natural linewidth of 0.1 GHz. Considering the Doppler width of the thermal muonium of 200 GHz, Lyman-α intensity of 4.6 $kW/cm^2$ is required to excite 25% of the ground state muonium to the 2P state. Thus, for a typical laser pulse duration of 4 ns and the muonium cloud cross-section of several square centimeters, Lyman-α pulse energies of approximately 10–100 μJ are required. Historically, the most commonly used method for generation in the vacuum-ultraviolet (VUV) region is the third harmonic generation (THG) in rare gasses. In general, however, the conversion efficiency of THG is relatively low because of the small value of the non-linear susceptibility for laser frequencies far from any resonance. Resonantly enhanced schemes, such as the sum-difference frequency mixing process, have conversion efficiencies that are several orders of magnitude higher [6,7]. The sum-difference frequency mixing process is illustrated in Fig. 1, where VUV is generated in a four-wave mixing process involving two photons at $\lambda_R = 212.55$ nm tuned to the two photon resonance of $4p^55p[1/2, 0]$ state of Kr and a third photon of tunable wavelength in the infrared (IR) region. Tuning of the IR laser to $\lambda_T = 820.9$ nm or $\lambda_T = 845.3$ nm results in the generation of Lyman-α for muonium or hydrogen, respectively. Using this scheme it is possible to generate VUV with large bandwidth using IR laser with large bandwidth that is matched to the 200 GHz doppler width of the thermal muonium produced from the hot tungsten foil. Recently, VUV pulse energies as high as 7 μJ at frequencies near Lyman-α were generated using the sum-difference frequency mixing process utilizing the two photon enhancement at 193 nm (resonant with $4p^56p[3/2,2]$ state) in Kr gas [8]. One of the major loss mechanisms in this process is photoionization of the excited Kr state by a third 193 nm photon or by the generated VUV photon. Since the photoionization rate from the $4p^55p[1/2, 0]$ state is lower than from $4p^56p[3/2,2]$ state it is preferable to use 212.55 nm radiation for the resonant enhancement in Kr [9,7].

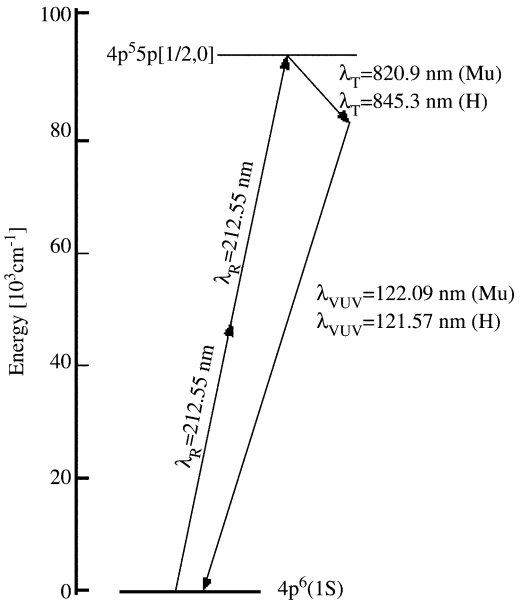


Fig. 1. Schematic diagram of resonantly enhanced sum-difference mixing process in Kr used to generate Lyman-α radiation for muonium and hydrogen.

## 2. Experimental setup

Owing to the short lifetime of 2P state of muonium (1.6 ns) and the nature of the frequency mixing process in Kr all lasers have to be synchronized to 1 ns accuracy. To achieve this level of accuracy the laser system is based on optical parametric oscillators (OPO) that have no intrinsic build-up time and are pumped by Nd:YAG lasers that have the build-up time jitter at only 1 ns level. The pumping Nd:YAG lasers are triggered in two stages. First, the flashlamps are triggered approximately 300 μs in advance of the ISIS muon pulse by delayed trigger from the previous muon pulse. The Q-switched pulses of the individual Nd:YAG lasers are then triggered to better than 1 ns accuracy from the current muon pulse. Flashlamp and Q-switch delays of the individual lasers are computer controlled and are independently adjusted to optimize the laser performance and timing relative to the muon pulse. In this way, the pulses of individual lasers can be synchronized to 1 ns accuracy with respect to each other as well as to the current muon pulse.

High power solid state lasers operating at high repetition rates suffer from poor beam quality due to high thermal load on the active medium, leading to stress induced birefringence and strong thermal lensing. This currently places a limit on the repetition rate of our laser system that is operating at only 25 Hz repetition rate, i.e. synchronized with only every second muon pulse.

A schematic diagram of our laser system is shown in Fig. 2. It consists of single-longitudinal mode (SLM) OPO oscillator with two-multipass Ti-sapphire amplifiers (Continuum Mirage 800) pumped by a frequency doubled, diode injection seeded, SLM Nd:YAG laser (Continuum Powerlite 9000). The Mirage 800 laser is tunable near 850 nm with bandwidth below 1 GHz and is producing output energies of 30–40 mJ/pulse. The output beam is further amplified in a 4-pass Ti:sapphire amplifier, longitudinally pumped by 650 mJ pulses from a frequency doubled Nd:YAG laser (Continuum Powerlite 9000), giving output energies of 150–200 mJ at 850 nm. After frequency doubling in a 7 mm long β-barium borate (BBO) crystal, pulse energies of up to 70 mJ at 425 nm are obtained. The wavelength of the 425 nm beam is monitored by a pulsed wavemeter (Burleigh WA-4500). The beam is then expanded with a telescope and split with a 50/50 beamsplitter before further frequency doubling in 5 mm long BBO crystals to 212.55 nm. The reason for this is twofold. Firstly, by reducing the incident energy, the heating effects caused by both linear absorption and non-linear absorption of 212.55 nm in BBO are reduced. This allows us to maintain the phase-matching condition over the cross-section of the beam. Secondly, two VUV beams can be generated independently in the Kr cell, where we also observed a strong saturation of the conversion process. As much as 6 mJ/pulse with pulse duration of 4 ns at 212.55 nm can be generated in each beam.

A broadband OPO laser coupled with an optical parametric amplifier (Continuum Mirage 3000) based on KTP is employed to generate the difference frequency between the excited $4p^5 5p[1/2, 0]$ state of Kr and the required Lyman-α frequency. The output is tunable from 815 to 855 nm allowing to generate Lyman-α for muonium, hydrogen and deuterium. The Mirage3000 laser is optically

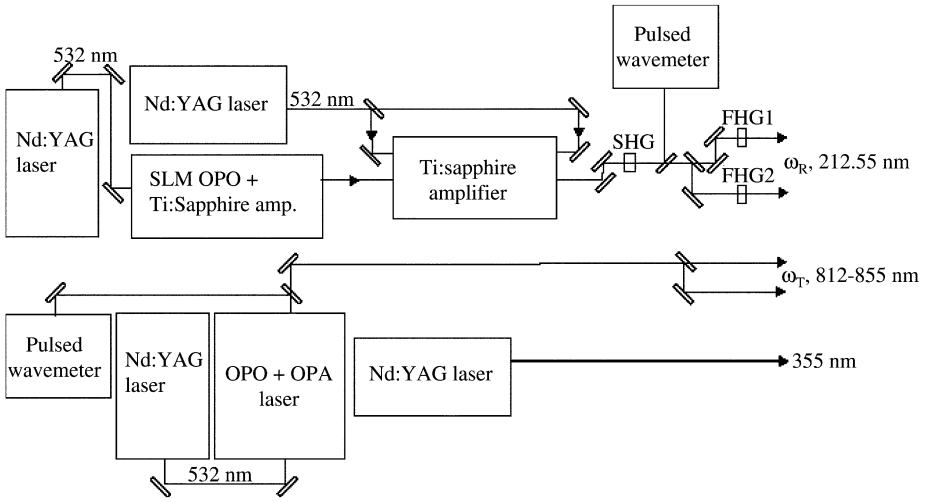


Fig. 2. Schematic diagram of the laser system. Certain elements such as telescopes and waveplates are for simplicity omitted from the diagram.

pumped by a frequency doubled Nd:YAG laser (Continuum Powerlite 7000). The resonator length of the OPO, the KDP crystal length as well as the focusing of the pump beam were optimized to generate the broad bandwidth output required for the efficient muonium ionization. The bandwidth, as measured by the Burleigh WA-4500 pulsed wavemeter, is typically 160 GHz (FWHM). The output pulse energy over the tuning range of the laser is typically 20 mJ with pulse duration of 12 ns.

Another frequency tripled Nd:YAG laser is used to generate 80 mJ pulses with 10 ns duration at 355 nm required for ionization of muonium from the 2P state.

The optical arrangement used for the generation of VUV radiation is shown in Fig. 3 together with the interaction area in front of the hot tungsten target. Two pairs of 212.55 nm and IR beams were used in some of our measurements to generate two VUV beams separated vertically by 20 mm. For simplicity only one beam is shown in Fig. 3. The 212.55 nm and IR beams are focussed separately to the 300 mm long Kr cell by 500 mm focal length lenses and combined collinearly by a dichroic mirror. The generated VUV beam is collimated in the horizontal plane by $f=125$ mm $MgF_2$ cylindrical plano-convex lens separating the Kr cell from the ultra-high vacuum in the target chamber of the slow muon beamline. The relative intensity of the generated VUV is monitored by measuring a photoionization current in an NO gas cell (at a pressure of 6.5 hPa) [11]. The muonium (or hydrogen) atoms excited by the Lyman-$\alpha$ beam to the 2P state are ionized by the pulsed 355 nm beam. This beam is introduced at an angle from the Lyman-$\alpha$ beam and retro-reflected at a small angle from the normal incidence to increase the interaction volume in front of the target. The total volume in front of the target defined by the overlap between the VUV and the 355 nm beam is estimated to be approximately 4 $cm^3$. A remotely controlled mirror with high reflectivity at 122 nm located in front of the NO cell can be used to retro-reflect the VUV beam(s).

Two stainless steel plates that can be translated in the horizontal and vertical direction, respectively, are mounted in front of the NO cell detector to determine the position and size of the VUV beam using the knife-edge method.

The surface muon beam with a flux of $5\times10^5$ $\mu^+/s$ enters the apparatus through a 50 $\mu$m thick stainless steel foil that is shielded from the high temperature tungsten target by a 25 $\mu$m thick

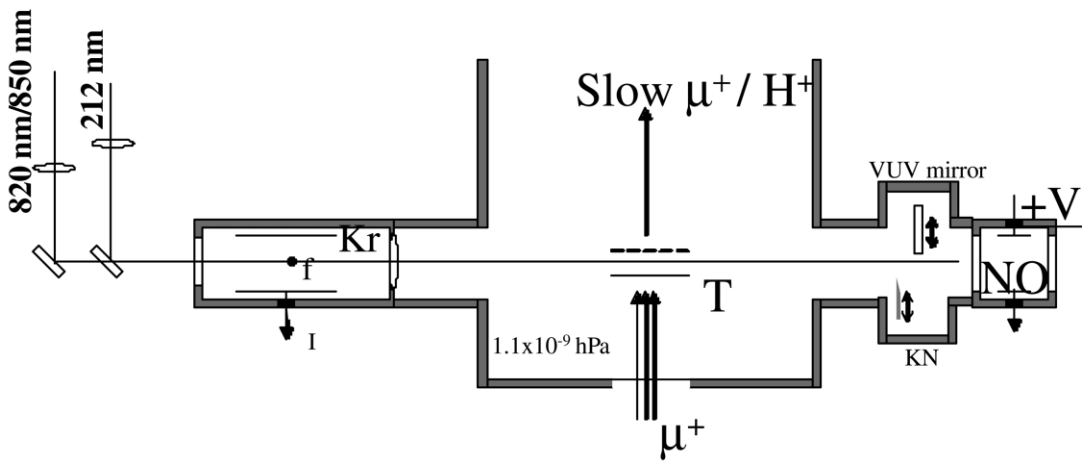


Fig. 3. Schematic diagram of the setup used for the VUV generation and of the muonium production target area. The 355 nm beam introduced from above the Kr cell at 45 degrees from the VUV beam is not shown. In this figure, Kr stands for Kr cell, T for tungsten target, NO for NO ionization cell, KN for motorized 'knife-edge' plate.

tungsten foil degrader. The target, a high purity (99.9999%) tungsten foil of 50 μm thickness, is located at the focus of the muon beam that was calculated to be of approximately 35 mm diameter. The target is heated to 2100 K by a d.c. current to maximize the muonium formation at the target surface. The laser pulses are triggered with a 0.4 μs delay after the pulse to allow for muonium propagation several millimetres away from the target.

The ionized particles are extracted by an immersion lens and transported through electrostatic quadrupoles, a bending magnet and electrostatic bend to a multichannel plate (MCP) detector [10]. The particle acceleration voltage can be adjusted between 0.5 and 10 kV. This slow muon transport beamline is evacuated down to ultra-high vacuum with three turbo pumps and a cryogenic pump. The bending magnet in the beamline enables separation of the extracted ions by their mass and thus select the type of particles transported to the MCP. The timing of the MCP signal, the muon beam trigger, as well as the timing of the laser pulses, and other relevant information were recorded with a CAMAC-based data acquisition system. The time-of-flight (TOF) of the particle through the beamline gives also a signature of the particle identity since particles of different mass will have different velocities at same acceleration voltage.

## 3. VUV generation in Kr and Ar gas mixtures

The generation of VUV in Kr was investigated under various experimental conditions. The confocal parameters of the incident beams could be varied over a wide range by using different lenses ($f=750$ mm, $f=500$ mm, $f=360$ mm) and two beam expanding telescopes.

The efficiency of the VUV generation depends primarily on the phase mismatch per Kr atom $C_{Kr}=\Delta k/N$ ($\Delta k=k_{VUV}-2k_R+k_T$), where $N$ is the number density of Kr atoms. In case of the two photon resonant difference frequency mixing in the wavelength region near Lyman-α the mismatch $C_{Kr}$ is negative [4]. An analysis of four wave mixing with different confocal parameters [12] has shown that in case of negative wave-vector mismatch ($\Delta k$), the maximum VUV energy is generated when $\Delta k=-2/b_R$. Thus, given the confocal parameter $b_R$ of the 212.55 nm beam and the phase mismatch per atom near Lyman-α ($C_{Kr}=-1.5\times10^{-17}$ cm$^2$), the maximum VUV signal should be observed for an optimum Kr pressure ($p_{opt}$) corresponding to $p_{opt}=-2\ K/(b_R\ C_{Kr})$,

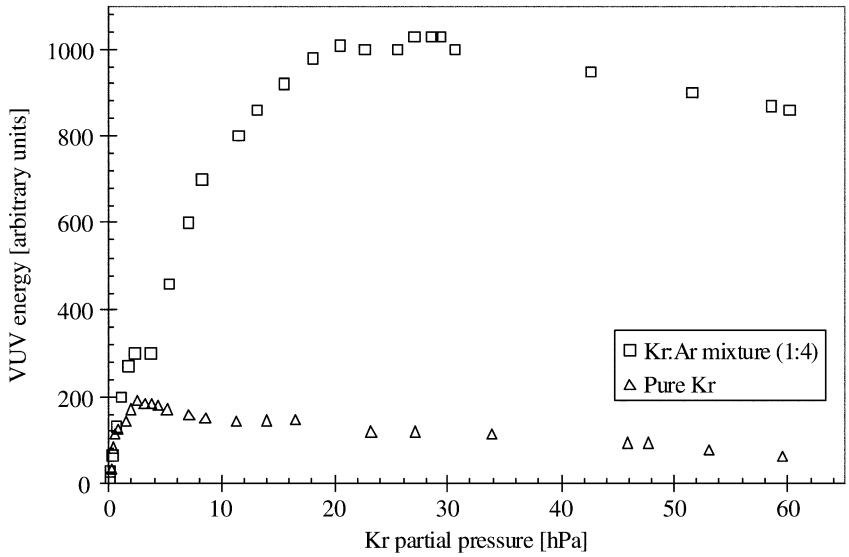


Fig. 4. Energy of hydrogen Lyman-α radiation generated in pure Kr gas and in phase-matched Kr–Ar mixture. Confocal parameters: $b_R = 3$ cm, $b_T = 2$ cm; energy of $\omega_R$ beam 3.6 mJ, energy of $\omega_T$ beam 5.6 mJ.

where $K = p_{Kr}/N_{Kr}$. This is in very good agreement with our experimental results when we observed the maximum VUV signal for $b_R = 4$, 2, and 0.5 cm at optimum Kr pressures 1.5, 2.5 and 11 hPa, respectively. Comparing the relative VUV energy for different confocal parameters, the largest value was observed for the weakest focusing tested ($b_R =$ 4 cm, $b_T = 5$ cm).

The wave vector mismatch limiting the VUV generation in pure Kr only to low number density can be compensated by using a buffer gas with a positive phase mismatch per atom in the Lyman-α region, such as Ar. In the limiting case of no absorption and ideal phase matching $\Delta k = 0$, the generated VUV energy should theoretically increase as a square of the Kr partial pressure [8,6]. Experiments performed by Marangos et al. at low input intensities and narrow bandwidth ($E_R = 0.18$ mJ and $E_T = 0.72$ mJ in pulses of 20 ns duration) have yielded an enhancement of the VUV energy in Kr–Ar mixture compared to optimum energy obtained in pure Kr of a factor of 100. Similar enhancement factor at Lyman-α frequency was observed in an experiment by Meyer et al. [13,8] using a different 2-photon resonance ($4p^5 6p[3/2,2]$ requiring $\lambda_R = 193$ nm). In both cases the increase of the VUV energy was found to be increasing proportionally to partial Kr pressure. Under our experimental conditions, however, the enhancement of the VUV energy with Ar gas phase-matching is observed to be rather modest. Fig. 4 shows the relative generated energy in pure Kr gas and in the Kr–Ar mixture measured at hydrogen Lyman-α frequency demonstrating an enhancement of a factor of only 5 due to a strong saturation effect with increasing pressure of Kr–Ar mixture. The data for VUV generation in Kr–Ar mixture at different Kr partial pressures were measured by preparing a phase-matched mixture at 60 hPa Kr base pressure and then evacuating the cell. The optimum phase-matching ratios between Kr and Ar were found to be 1:4.0 and 1:5.8 for 121.57 nm (hydrogen) and 122.09 nm (muonium), respectively. The VUV energy, as shown in Fig. 4 was found to have a maximum at relatively low Kr pressure of 20 hPa.

We have investigated the dependence of the saturation pressure on some experimental conditions. We have found that the saturation pressure stays constant over a wide range of the incident energies of the 212.55 nm beam, from 0.1 to 3.5 mJ. The change of confocal parameters has also

had only a limited effect on the value of the saturation pressure and has not yielded any significant increase in the observed VUV energy.

A measurement of dependence of the VUV yield on the input energy of $\omega_T$ beam has revealed a strong saturation, which occurs at energies as low as 1 mJ/pulse. The saturation energy of $\omega_T$ depends on the energy of $\omega_R$ and can be increased by increasing the energy of $\omega_R$. For example at $E_R = 5$ mJ/pulse, $b_R = 0.5$ cm and $b_T = 0.4$ cm the saturation energy of $\omega_R$ increases to 7 mJ/pulse.

Fig. 5 shows the dependence of the VUV signal on Kr partial pressure in the phase-matched Kr–Ar mixture measured at low energy of $\omega_R$ and several energies of $\omega_T$. The measurements demonstrate that with increasing $\omega_T$ energy the saturation effects limiting the VUV generation are stronger and that the saturation pressure at which the VUV output is maximized changes significantly.

There are several saturation and loss mechanisms which contribute to saturation at high energies, such as 3-photon ionization, two-photon re-absorption [7], amplified spontaneous emission from $4p^55p[1/2,0]$ state [14], stimulated hyper-Raman scattering, self-defocusing [15] and other non-linear effects. This results in either change of population distribution and related changes of refractive index that can lead to loss of phase matching, or to a direct depletion of the generated VUV beam or the incident $\omega_T$ and $\omega_R$ beams. At present we have no model that would consider all of the saturation and phase mismatch effects and explain the observed saturation behavior. Judging from the data in Fig. 5 and from the strong saturation of the VUV yield with increasing $\omega_T$ energy a large contribution to the saturation is likely to come from two photon resonant re-absorption of VUV. The sum of the photon energies of the VUV and the $\omega_T$ are inherently equal to $2\omega_R$ and the two-photon absorption is thus resonantly enhanced. The saturation of the VUV signal with increasing power of $\omega_T$, which could be attributed to the two photon absorption, was also observed by Hilber et al. [7] in a resonantly enhanced sum-difference mixing experiment using $4p^55p[5/2,2]$ transition ($\lambda_R = 216.6$ nm) in Kr, as well as in our earlier experiment at KEK [4].

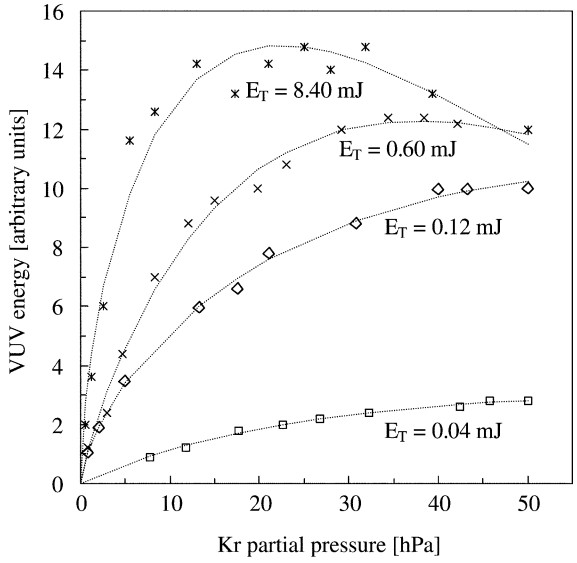


Fig. 5. Dependence of the VUV pulse energy on the Kr partial pressure (Kr:Ar = 1:4) measured at low energy of 212.55 nm beam ($E_R = 0.2$ mJ) and several energies, $E_T$, of the IR beam at $\lambda_T = 844.9$ nm. Confocal parameters of the input beams are $b_R = 0.8$ cm, and $b_T = 1$ cm. Dashed lines represent fit to the data in the form of $\alpha p_{Kr}^{\beta}\exp(-\gamma p_{Kr})$, where $\alpha$, $\beta$, and $\gamma$ are the fitting parameters.

Considering the relatively broad bandwidth of our $\omega_T$ beam, the VUV generation can be, in principle, also limited by low acceptance bandwidth of the Kr–Ar mixture at higher pressures. The actual acceptance bandwidth depends on the shape of the phase matching integral that has maximum at $\Delta k = 0$ and can be approximated as $\exp(b_R\Delta k)$ for $\Delta k \leqslant 0$ and as $\exp(-b_T\Delta k)$ for $\Delta k \geqslant 0$ [8]. The acceptance bandwidth for large confocal parameters of the input beams could be expected to be of a comparable size to the $\omega_T$ bandwidth at relatively low Kr pressure. To check whether this is the case, we have measured the VUV tuning range at the Kr partial pressure of 50 hPa in the phase-matched mixture near 212.5 nm (Fig. 6). Though at this pressure the VUV signal was strongly saturated, the tuning range measured at full-width half-maximum was 0.45 nm. This is more than an order of magnitude larger than the bandwidth of the $\omega_T$ beam (or the VUV beam) and we can conclude that the VUV yield

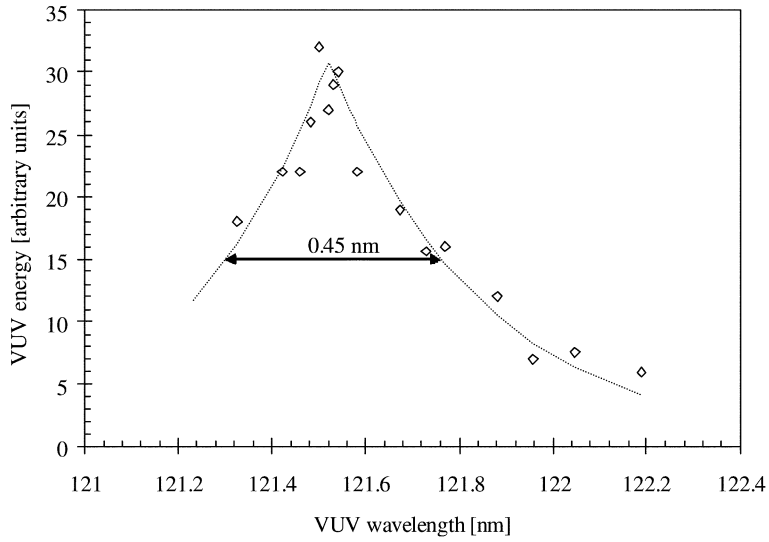


Fig. 6. Measured tuning range near hydrogen Lyman-α wavelength using a phase-matched Kr–Ar mixture at a Kr partial pressure of 50 hPa. The dashed line represents a fit to the data with an approximated phase matching integral—see text. Confocal parameters: $b_R = 0.8$ cm, $b_T = 1$ cm; energy of $\omega_R$ beam 3.6 mJ, energy of $\omega_T$ beam 5.6 mJ.

saturation at this pressure is not due to the narrow acceptance bandwidth for phase-matching. The full tuning range on the high frequency side could not be measured due to the limited tuning range of our broadband OPO laser. The phase matching profile was fitted with the expected shape of the phase matching integral discussed above. The ratio of the confocal parameters giving the best fit to the data is $b_R/b_T = 0.9$.

## 4. Hydrogen ionization

The whole experimental setup, including the laser system, ion transport beamline, and MCP detector, was tested by ionizing hydrogen atoms in front of the tungsten target. Given the capability of the setup to detect single particles, the experiment was performed using residual hydrogen in the ultra-high vacuum without introducing any additional $H_2$ gas. The hydrogen atoms are produced by dissociation from $H_2$ on the surface of the heated tungsten target with maximum efficiency at target temperatures above 2000 K [4]. $H^+$ ions were transported to the MCP with a characteristic TOF delay relative to the laser pulses and characteristic mass corresponding to protons. Up to $10^5$ $H^+$ were observed per laser pulse from an ionization volume of approximately 4 $cm^3$ at ultra-high vacuum pressures of only $1.1\times10^{-9}$ hPa. Only one VUV beam without the VUV retro-reflecting mirror was used for these measurements. The VUV intensity can be increased by a factor of three if both VUV beams and the retro-reflection mirror are used.

We have also measured the value of the Lyman-α wavelength to check calibration of our wavemeters. Fig. 7 shows the measured yield of laser ionized hydrogen as a function of VUV wavelength near 121.6 nm. The VUV wavelength was determined from direct measurements of $\omega_R/2$ and $\omega_T$ using a pulsed wavemeter. The measured center wavelength of 121.568 nm is in very good agreement with the theoretical Lyman-α wavelength (121.5676 nm). The measured line profile is a convolution of the Doppler profile of hydrogen at 1900 K, with FWHM of 78 GHz, and of the Lorentzian profile of the OPO laser output. The data were therefore fitted with a Voigt profile. The linewidth measured at FWHM is 122 GHz. This is lower than the bandwidth of the OPO laser (160 GHz) indicating possible line narrowing in the VUV generation process.

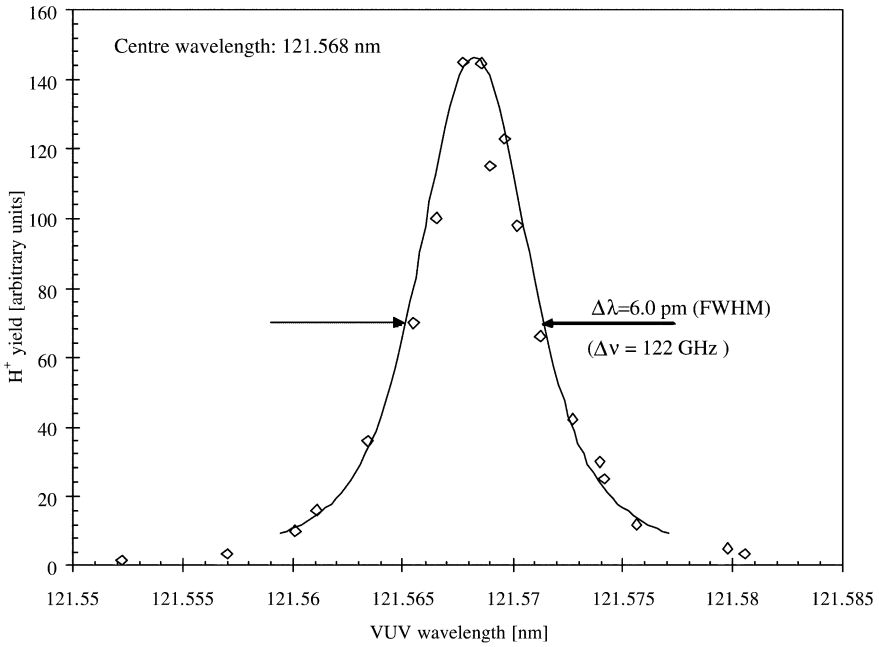


Fig. 7. Yield of laser ionized hydrogen detected on the MCP as a function of wavelength near 121.6 nm. Solid line represents a Voigt profile fit to the measured data.

## 5. Slow muon generation

The slow muon generation experiment was carried out in the summer of 2001 for 5 days. The surface of the tungsten target was cleaned in oxygen atmosphere with $4\times10^{-7}$ hPa pressure at 1800 K for 8 h before the start of the experiment when the temperature was increased to 2000 K for the muonium production.

The muon pulse repetition rate at the ISIS facility is 50 Hz, twice the repetition rate of the laser system. This allowed us to make easily measurements with and without the laser ionization. An observed TOF spectrum is shown in Fig. 8. A clear signal appeared only when the VUV light was introduced in front of the target, and the observed peak was confirmed to correspond to the calculated TOF for slow muons at the acceleration voltage of 7.5 kV. Time $t=0$ in Fig. 8 was chosen to be 120 ns prior to the laser Q-switch trigger, so that the Q-switch trigger could be recorded simultaneously. Time jitter of 20 ns originating in the data acquisition system was observed on both the Q-switch trigger signal and the slow muon signal. The measured width of the slow muon peak in the TOF spectrum is limited by this jitter. The real width is expected to be about a factor of two smaller. The electric field gradient of 100 V/cm in front of the target introduces an additional uncertainty on the energy of the particles detected at the MCP position. The extraction energy of the $\mu^+$ depends on the distance from the target at which the muonium is ionized. For the VUV beam diameter of 8 mm this effect introduces an energy uncertainty of 80 eV and respective TOF uncertainty of 7.5 ns.

If required, this energy uncertainty can be reduced by reducing the size of the VUV beam and by reducing the electric field gradient in front of the target. Reduction of the energy uncertainty to below 10 eV should be achievable without significant loss in the number of slow muons that are generated and extracted from the target area. The VUV pulse energies generated by the laser

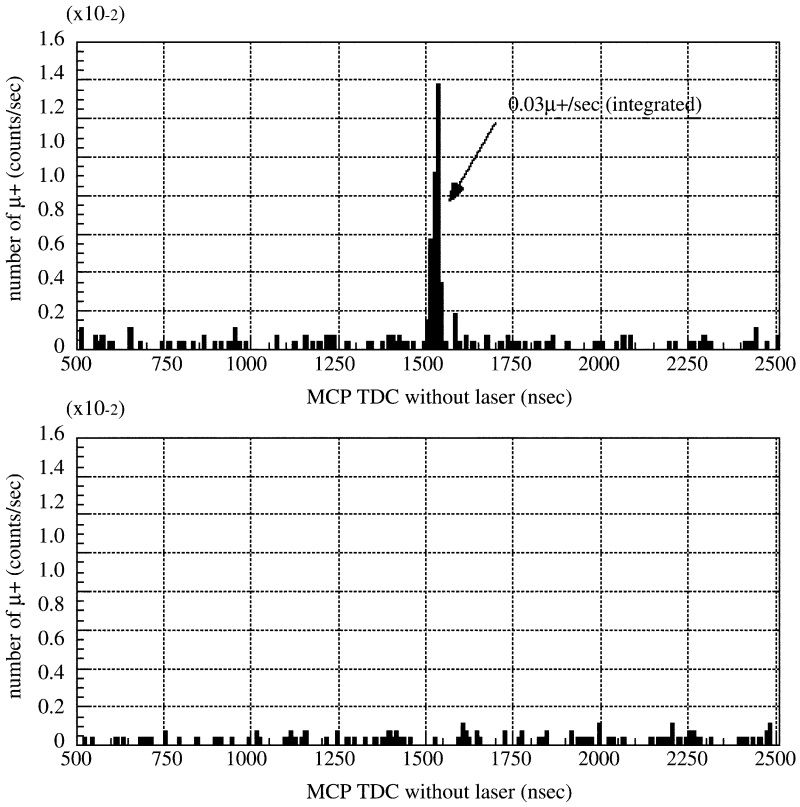


Fig. 8. Comparison of slow muon TOF spectrum measured with and without the laser ionization. The beamline acceleration voltage was 7.5 kV.

system are currently not high enough to saturate the 1S–2P transition. Therefore, the reduction of the number muonium atoms in a more focused laser beam would be compensated by the increased ionization efficiency.

The muonium yield was also measured as a function of the difference wavelength $\lambda_T$. Maximum yield of slow muons was observed for $\lambda_T =$ 821.1 nm corresponding to the generated VUV wavelength of 122.08 nm. This is in agreement with the expected 1S–2P transition frequency in muonium (122.0891 nm). We have also scanned the timing of laser pulses relative to the incoming muon pulse. It was found that the yield is maximized when the laser is introduced 0.4 μs after the muon pulse. This agrees with previous experiments on muonium production from hot metal surfaces [3].

## 6. Conclusion

Generation of ultra-slow muon beam from pulsed surface muon beam using two photon resonant laser ionization of muonium was demonstrated. The measured yield of 0.03 $\mu^+/s$ obtained during the first beamtime is currently below the design value for this apparatus. Unfortunately, the design of our apparatus does not currently allow us to measure the absolute muonium production and the absolute VUV energy independently. It is therefore difficult to determine the exact reason for the low slow muon yield.

The hydrogen ionization measurements have shown that up to $10^5$ $H^+$ per pulse can be obtained at a vacuum level $1.1\times10^{-9}$ hPa. Assuming that the pressure corresponds to free hydrogen atoms only, we can estimate the combined ionization and detection efficiency to be better than $10^{-3}$. Assuming the surface muon beam intensity of $5\times10^5$ $\mu^+/s$, the efficiency of conversion to muonium of 2%, fraction of the muonium in the laser beam of 50%, and decay of 50% of the muons in flight, we can then expect slow muon yield of the order 1 $\mu^+/s$.

The discrepancy is likely to be due to low efficiency of muonium production. An improvement can be expected from experimental tuning of the momentum of the initial muon beam to match the thickness of the target. Relative muonium yield as a function of the muon beam momentum can be, in principle, measured by the laser ionization in our apparatus. We have also found that a beam collimator placed on the input of our apparatus was partly blocking the muon beam and contributed to the reduction of the observed slow muon signal. The slow muon signal showed almost linear dependence on energies of both VUV and the 355 nm pulses, suggesting that significant improvement can be gained by improving the efficiency of VUV generation.

Further work is in progress to better understand the saturation processes involved in the generation of the intense VUV radiation in phase-matched gas mixtures of Kr and Ar and to install a calibrated VUV detector to measure the absolute energy of the generated VUV pulses.

## Acknowledgments

The authors would like to acknowledge Drs K. Ishida, T. Matsuzaki, and I. Watanabe for their contributions to the construction of the experimental set-up, and Dr Marangos for helpful discussions on the subject of VUV generation. The authors would like to thank Mr Fujino and Mr Shiraishi for their contribution to the building of the laser system. This research was partially supported by the Japanese Ministry of Education, Science, Sports and Culture, Grant-in-Aid for Scientific Research (B), 2000, 11559019.

## References

[1] E. Morenzoni, in: S. Lee, S. Likcoyne, R. Cywinski (Eds.), Muon Science, Institute of Physics Publishing, 1999, pp. 343–404.

[2] E. Morenzoni, H. Glückler, T. Prokscha, H.P. Weber, E.M. Forgan, T.J. Jackson, H. Luetkens, Ch. Niedermayer, M. Pleines, M. Birke, A. Hofer, J. Litterst, T. Riseman, G. Schatz, Low-energy μSR at PSI: present and future, Physica B 289–290 (2000) 653–657.

[3] A.P. Mills Jr, J. Imazato, S. Saitoh, A. Uedono, Y. Kawashima, K. Nagamine, Generation of thermal muonium in vacuum, Phys. Rev. Lett. 56 (14) (1986) 1463–1466.

[4] Y. Miyake, J.P. Marangos, K. Shimomura, P. Birrer, T. Kuga, K. Nagamine, Laser system for the resonant ionization of hydrogen-like atoms produced by nuclear reactions, Nucl. Instr. Meth. Phys. Res. B 95 (1995) 265–275.

[5] T. Matsuzaki, K. Ishida, K. Nagamine, I. Watanabe, G.H. Eaton, W.G. Williams, The RIKEN-RAL pulsed muon facility, Nucl. Instr. Meth. Phys. Res. A 465 (2–3) (2001) 365–383.

[6] J.P. Marangos, N. Shen, H. Ma, M.H.R. Hutchinson, J.P. Connerade, Broadly tunable vacuum-ultraviolet radiation source employing resonant enhanced sum-difference frequency mixing in krypton, J. Opt. Soc. Am. B 7 (7) (1990) 1254–1259.

[7] G. Hilber, A. Lago, R. Wallenstein, Broadly tunable vacuum-ultraviolet/extreme-ultraviolet radiation generated by resonant third-order frequency conversion in krypton, J. Opt. Soc. Am. B 4 (1987) 1753–1764.

[8] G.W. Faris, S.A. Meyer, M.J. Dyer, M.J. Banks, Two-photon-resonant difference frequency mixing with an ArF excimer laser: vacuum-ultraviolet generation and multiphoton spectroscopy, J. Opt. Soc. Am. B 17 (11) (2000) 1856–1866.

[9] K. Miyazaki, H. Sakai, T. Sato, Two-photon resonances in Xe and Kr for the generation of tunable coherent extreme UV radiation, Appl. Opt. 28 (4) (1989) 699–702.

[10] Y. Miyake, K. Shimomura, Y. Matsuda, R.J. Scheuermann, P. Bakule, S. Makimura, P. Strasser, S.N. Nakamura, K. Ishida, T. Matsuzaki, I. Watanabe, K. Nagamine, Construction of the experimental set-up for ultra slow muon generation by thermal Mu ionization method at RIKEN-RAL, Physica B 289–290 (2000) 666–669.

[11] J.A.R. Samson, Techniques of vacuum ultraviolet spectroscopy, Wiley Series in pure and applied spectroscopy, New York; London, 1967.

[12] G. Hilber, D.J. Brink, A. Lago, R. Wallenstein, Optical-frequency conversion in gases using Gaussian laser beams with different confocal parameters, Phys. Rev. A 38 (12) (1988) 6231–6239.

[13] S.A. Meyer, G.W. Faris, High power Lyman-α source generated with an ArF excimer laser, Opt. Lett. 23 (3) (1998) 204–206.

[14] J.C. Miller, 2-photon resonant multiphoton ionization and stimulated-emission in krypton and xenon, Phys. Rev. A 40 (12) (1989) 6969–6976.

[15] H. Scheingraber, C.R. Vidal, Saturation of resonant 3rd harmonic generation due to self-defocusing and a redistribution of the population densities, IEEE J. Quant. Electron. 19 (1983) 1747–1758.